The excitation of $N_2(B\,^3\Pi_g, v=1\text{–}12)$ in the reaction between $N_2(A^3\Sigma_u^+)$ and $N_2(X, v\geqslant 5)$

Lawrence G. Piper
Physical Sciences Inc., Research Park, P. O. Box 3100, Andover, Massachusetts 01810-7100

(Received 18 January 1989; accepted 6 April 1989)

We have studied the excitation of $N_2(B\,^3\Pi_g, v = 1\text{–}12)$ in the interaction between $N_2(A\,^3\Sigma_u^+)$ and $N_2(X\,^1\Sigma_g^+, v\geqslant 5)$. The $N_2(A)$ and $N_2(B)$ are observed spectroscopically between 220 to 400 nm and 560 to 900 nm, respectively, while the $N_2(X,v)$ number densities are determined by metastable-helium Penning ionization. The experiments are performed in a discharge-flow reactor with separate discharge sources of $N_2(A)$, $N_2(X,v)$ and $He^*(2^3S)$. The excitation rate coefficient is $(3 \pm 1.5)\times 10^{-11}$ cm^3 molecule^{-1} s^{-1}. Observations of $N_2(A)$ decay indicate that the $N_2(A)$ is removed by $N_2(X,v)$ with an apparent rate coefficient of about 3.5×10^{-12} cm^3 molecule^{-1} s^{-1}. The discrepancy between the excitation and removal rate coefficients probably results from $N_2(A)$ regeneration via cascade from the excited $N_2(B)$. The appearance of vibrationally excited $N_2(A)$ when $N_2(X,v)$ is added to a flow of $N_2(A, v = 0)$ demonstrates this regeneration process. The reaction appears to be a transfer of electronic energy from the $N_2(A)$ to the $N_2(X,v)$ rather than an excitation of the $N_2(A)$ to $N_2(B)$ resulting from the input of energy from the $N_2(X,v)$.

I. INTRODUCTION

A number of researchers have speculated on a possible energy pooling reaction between $N_2(A\,^3\Sigma_u^+)$ and $N_2(X\,^1\Sigma_g^+,v)$ to generate $N_2(B\,^3\Pi_g)$.[1–5] This speculation has been fueled to some extent by observations of long-lived $N_2(B)$ radiation in discharge afterglows. For the most part, however, the observations also could be explained by alternative mechanisms. To our knowledge, there is a complete dearth of direct experimental evidence for this reaction. We report here a direct observation of the reaction, with estimates of its efficiency.

Our observations cover the range of $N_2(B)$ vibrational levels 1–12. The energetics of the reaction are such that $N_2(X)$ vibrational levels between 5 and 14 are required to excite the observed B-state levels from $N_2(A, v = 0)$. Observations of enhanced B-state emission upon adding $N_2(A)$ to an active nitrogen afterglow, therefore, provide a diagnostic of these moderately energetic ground-state vibrational levels. We have explored previously the application of metastable-helium Penning ionization as a diagnostic of $N_2(X,v)$,[6,7] and showed that this diagnostic could provide quantitative estimates of number densities in vibrational levels 0–6.[7] Our current research is directed toward developing a diagnostic of higher vibrational levels.

II. EXPERIMENTAL

These studies employed the 4.6 cm diameter quartz discharge-flow reactor shown schematically in Fig. 1. $N_2(A)$, generated by energy transfer between metastable-argon atoms and molecular nitrogen,[8,9] enters the reactor at its upstream end and mixes further downstream with a flow of vibrationally excited, ground-electronic state, nitrogen molecules. The $N_2(X,v)$ is prepared in a sidearm and introduced into the reactor through a hook-shaped injector. A 0.5 m monochromator equipped with photoelectric detection capability detects the luminescence generated in the reaction further downstream from the $N_2(X,v)$ injector. The monochromator is mounted on rails so that observations can be made at various distances from the injector, and thereby various interaction times. A second injector further downstream disgorges a flow of metastable helium atoms which reveal the presence of $N_2(X,v)$ via a Penning-ionization reaction.[6,7,10,11]

A hollow-cathode, dc discharge through a flow of 3%–10% argon in helium generates metastable argon atoms. The argon metastables mix immediately downstream from the discharge with a flow of nitrogen. The argon metastables excite $N_2(C\,^3\Pi_u)$ which immediately radiates to the $N_2(B)$ state. Radiation and quenching of the B state then results in $N_2(A)$-state production. The number densities of $N_2(A)$ generated in the predominantly helium buffer are similar to those obtained in a pure argon buffer. The $N_2(A)$ vibrational distribution, however, tends to be slightly more relaxed because helium is much more efficient than argon at relaxing the vibrational energy in the A state.[12]

A microwave discharge through a flow of nitrogen in helium, or just pure nitrogen generates the $N_2(X,v)$. Downstream from the discharge, the active nitrogen flows through a nickel screen. The screen recombines most of the atoms and, in addition, deactivates electronically excited metastables produced in the discharge. It has little effect of the $N_2(X,v)$, however.[7,13] Failure to observe Lewis–Rayleigh afterglow downstream from the nickel screen demonstrates the absence of N atoms. The $N_2(X,v)$ is introduced into the main flow after atom recombination and metastable deactivation have occurred.

A hollow-cathode, dc discharge in the upstream portion of the second injector generates metastable-helium atoms. The Penning ionization of N_2 produces $N_2^+(B\,^2\Sigma_u^+)$ which is observed readily in emission on the nitrogen first-negative system, $N_2^+(B\,^2\Sigma_u^+)$–$X\,^2\Sigma_g^+$). The vibrational distribution

 0021-9606/89/140864-10$02.10

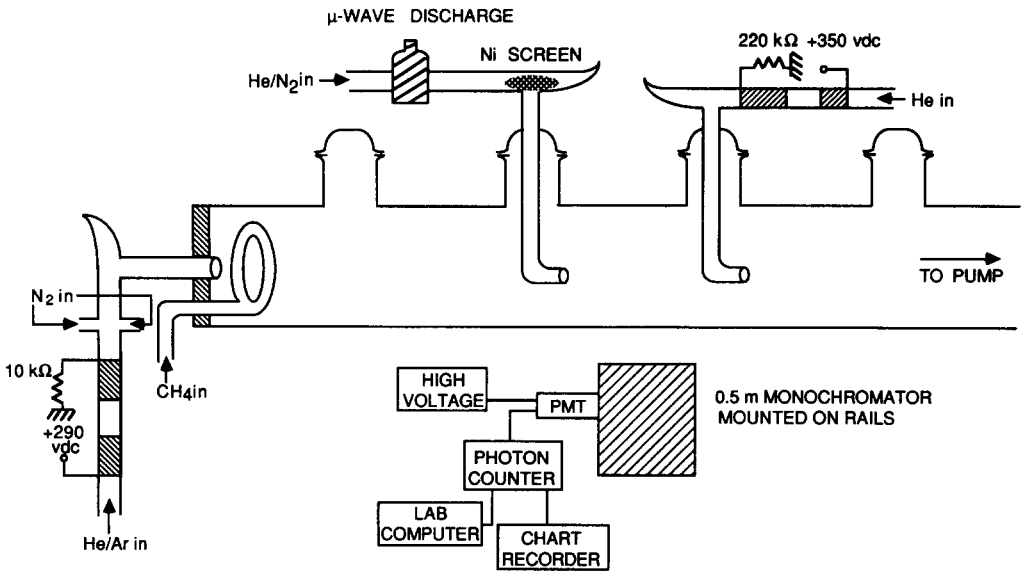

FIG. 1. Schematic of discharge-flow apparatus for studying $N_2(A)$ and $N_2(X,v)$.

of $N_2^+(B)$ mirrors that of the $N_2(X,v)$ from which it was generated. We have described in some detail previously our procedures and analysis relating to monitoring $N_2(X,v)$ using a Penning-ionization diagnostic.[6,7] Our previous work indicated that $N_2(X,v)$ was deactivated only very slowly in collisions with the reactor walls. The $N_2(X,v)$ distributions as determined by Penning ionization downstream from the second hook injector, therefore, ought to be a reasonable reflection of the actual distributions within the observation zone just downstream from the first hook injector. We tested this conjecture experimentally in the present series of experiments by comparing the $N_2(B)$ distribution and intensity immediately downstream from the $N_2(X,v)$ injector with that observed downstream from the metastable-helium injector. The results at the two locations, after correcting for differences in $N_2(A)$ number densities, were the same.

The relative spectral response of our detection system was calibrated by comparing observed intensity distributions as a function of wavelength with those emitted by standard quartz–halogen and deuterium lamps. Light from the lamps was reflected into the monochromator off a $BaSO_4$ screen[14] so as to ensure that the optics were filled. The response was calibrated absolutely at 538 nm by comparison with air-afterglow intensities.[15–21] We have detailed our procedures for making air-afterglow calibrations previously.[22,23]

With the detection system calibrated absolutely, we could determine absolute number densities of all emitting species by dividing absolute band intensities by the appropriate Einstein coefficients. The spectral fitting procedure we have described previously determined the band intensities. Shemansky's[24] Einstein coefficients were used to reduce $N_2(A)$ observations while those of Piper *et al.*[25] were used for $N_2(B)$.

Mass-flow meters or rotameters monitored the flow rates of all gases. The calibrations of all mass-flow meters and most rotameters were checked by monitoring the pressure rise with time in a calibrated volume. Some of the rotameters were calibrated by comparison with a calibrated mass-flow meter. This was done by establishing the dependence of flow-tube pressure on gas-flow rate using the calibrated mass-flow meter for flow-rate measurements. This correlation could then be used to derive flow rates of the uncalibrated flow meter from measurements of flow tube pressure for various flow-meter settings. A capacitance manometer monitored the flow-tube pressure.

Typical conditions included main flow of 2500 to 5000 μmol s^{-1}, flow of helium and N_2 through the $N_2(X,v)$ injector of 275 and 140 μmol s^{-1} respectively, and flow of helium through the He* injector of 1600 μmol s^{-1}. In some instances flows of methane were added to the flow of $N_2(A)$, at flow rates up to 90 μmol s^{-1}, in order to relax the vibrational energy in the $N_2(A)$.[26,27] Flow tube pressures ranged between 0.9 and 3.3 Torr.

III. RESULTS

A. $N_2(B)$ excitation

When the discharges producing $N_2(A)$ and $N_2(X,v)$ are both on, one sees an orange afterglow streaming from the $N_2(X,v)$ injector. When either discharge is extinguished the afterglow vanishes. Figure 2 shows the spectrum, with $N_2(X,v)$ in the reactor, between 560 and 900 nm in the presence and absence of $N_2(A)$. Quite strong nitrogen first-positive emission, $N_2(B\,^3\Pi_g - A\,^3\Sigma_u^+)$, obtains with the addition of $N_2(A)$ while radiation is undetectable in the absence of $N_2(A)$. The $N_2(A)$ number densities were sufficiently small and the spectrometer slit widths sufficiently narrow that $N_2(B)$ formed by $N_2(A)$ energy pooling[28] was unobservable.

Figure 3 shows that the intensity of the 2,0 band of the first-positive system varies linearly with the intensity of the Vegard–Kaplan system, $N_2(A\,^3\Sigma_u^+ - X\,^1\Sigma_g^+)$. Since the Vegard–Kaplan intensity is directly proportional to $N_2(A)$ number density, these results show that the $N_2(B)$ excitation is first order in $N_2(A)$ number density.

We have shown previously that $N_2(X,v)$ number densities vary,[7(b)] although not linearly, with discharge power.

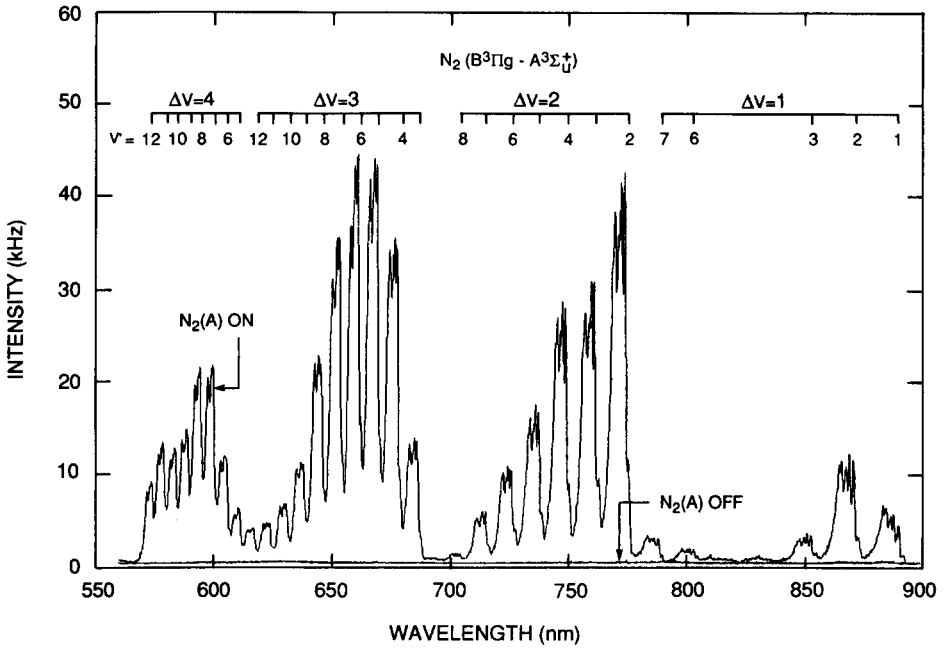

FIG. 2. Spectrum of nitrogen first-positive bands, $N_2(B\,^3\Pi_g - A\,\Sigma_u^+)$, excited in the reaction between $N_2(A)$ and $N_2(X,v)$. The baseline shows the spectrum in the absence of $N_2(A)$. The spectrum has not been corrected for relative spectral response.

The number densities increase fairly rapidly as the power is increased to ~50 W, but appear to level off around 70 W. Figure 4 shows how the observed $N_2(B)$ number densities vary with discharge power. In this set of experiments, the discharge power was varied under otherwise constant conditions of flow rates and $N_2(A)$ number density. We interpret the similarity between the variations in $N_2(B)$ with discharge power and our previous observations on $N_2(X,v)$ production with discharge power as strong evidence for $N_2(B)$ generation in the reaction between $N_2(A)$ and $N_2(X,v)$.

These observations can be rationalized by the following reactions which govern the formation and destruction of $N_2(B)$:

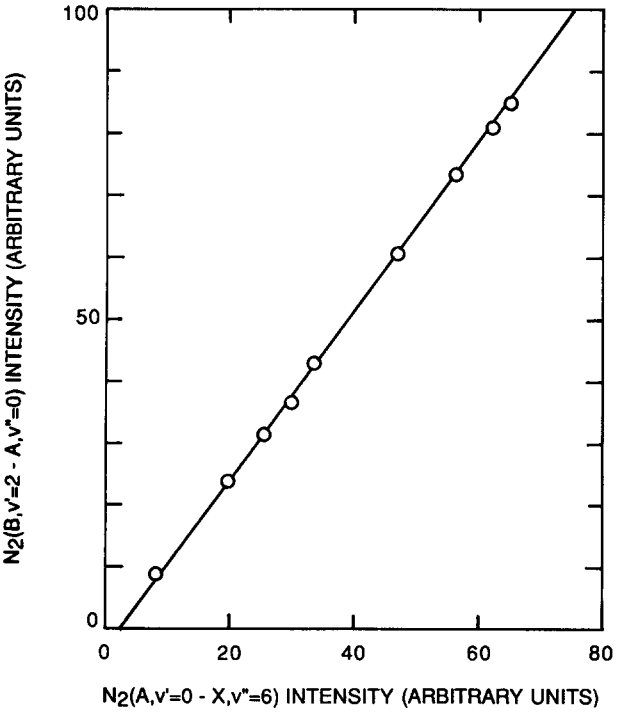

FIG. 3. Variation in the intensity of the 2,0 band of the first-positive system as a function of the intensity of the 0,6 band of the nitrogen Vegard–Kaplan system $N_2(A\,^3\Sigma_g^+ - X\,^1\Sigma_g^+)$.

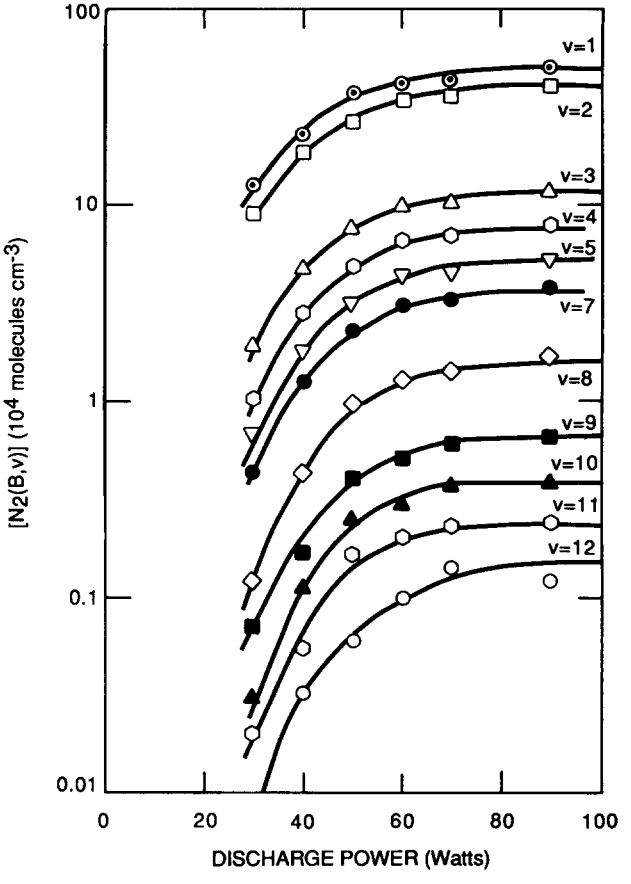

FIG. 4. Variation in the number density of different vibrational levels of $N_2(B)$ as a function of the power of the μ-wave discharge under conditions of constant $N_2(A)$ number density. $N_2(X,v)$ number densities scale with discharge power in a manner similar to the $N_2(B,v)$ in this figure.

$$N_2(A\,^3\Sigma_u^+) + N_2(X\,^1\Sigma_g^+,v) \rightarrow N_2(B\,^3\Pi_g,v') + N_2(X\,^1\Sigma_g^+,v''), \quad (1)$$

$$N_2(B\,^3\Pi_g) \rightarrow N_2(A\,^3\Sigma_u^+) + h\nu, \quad (2)$$

$$N_2(B\,^3\Pi_g) + N_2 \rightarrow 2N_2, \quad (3)$$

$$N_2(B\,^3\Pi_g) + Q \rightarrow N_2(X) + Q. \quad (4)$$

Both the radiative decay rate[25,29] of $N_2(B)$ and the rate coefficient for quenching $N_2(B)$ by nitrogen are vibrational-level dependent.[28,30–32] To analyze our data we use average values for these quantities: $k_2 \sim 2\times10^5$ s^{-1} and $k_3 \sim 2.5\times10^{-11}$ cm^3 molecule^{-1} s^{-1}.

The quenching of $N_2(B)$ by molecular nitrogen is a complex process with the likely production of a number of states including $N_2(W^3\Delta_u)$, $N_2(B'^3\Sigma_u^-)$, $N_2(A\,^3\Sigma_g^+,v)$. Reaction (3), therefore, encompasses all possibilities. It accounts for removal of molecules from the B state. Ultimately most of the B-state quenching by N_2 probably results in cascade down through the triplet manifold to the A-state.

Reaction (4) accounts for possible quenching of the $N_2(B)$ fluorescence by methane, argon, and helium. The argon partial pressure generally was well below 75 mTorr, whereas the half-quenching pressure for argon is greater than 1 Torr.[33,34] Thus quenching by argon should be less than a 10% effect. Our observations on the excitation of $N_2(B)$ in the reaction between $N(^2D)$ and $NF(a\,^1\Delta)$[35] indicated a half-quenching pressure for helium of about 5 Torr. Thus quenching by helium at pressures near 1 Torr is a minor, but not insignificant, loss process for $N_2(B)$. The partial pressure of methane remained below 25 mTorr. So long as the rate coefficient for quenching $N_2(B)$by methane is no greater than 3×10^{-11} cm^3 molecule^{-1} s^{-1}, i.e., is less than one-tenth gas kinetic, methane quenching will be unimportant for our studies. Bayes and Kistiakowsky[36] indicate that methane does quench $N_2(B)$ emission, but they failed to provide any estimate of its quenching efficiency. We are unaware of any other observations of $N_2(B)$ quenching by methane. We could not distinguish any strong dependence of the $N_2(B)$ fluorescence yield upon methane number density, so conclude that methane quenching is indeed of little importance in our studies.

The differential equation describing the rates of formation and destruction of $N_2(B)$ as governed by the processes in Eqs. (1)–(4) is

$$\frac{d[N_2(B)]}{dt} = k_1[N_2(A)][N_2(X,v)] - \{k_2 + k_3[N_2] + k_4[Q]\}[N_2(B)]. \quad (5)$$

Because the radiative lifetime of $N_2(B)$ ($\sim 5\,\mu$s)[29] is much shorter than the transit time through our detector's field of view, the $N_2(B)$ is in local steady state at every point in our reactor. The variation in $[N_2(B)]$ with time vanishes, therefore, and Eq. (5) can be rearranged to give

$$[N_2(B)] = \frac{k_1[N_2(A)][N_2(X,v)]}{k_2 + k_3[N_2] + k_4[Q]}. \quad (6)$$

This equation demonstrates the first-order dependence between $N_2(B)$ excitation and the number densities of $N_2(A)$ and $N_2(X,v)$.

In order to observe how the $N_2(B)$ excitation varied with $N_2(A)$ vibrational level, we mixed varying amounts of methane with the total $N_2(A)$ at the head of the flow reactor. The added methane appeared to affect the total $N_2(A)$ number density only minimally, but reduced the $N_2(B)$ intensity by more than a factor of 2.5 as the methane number density was increased to 7.5×10^{14} molecules cm^{-3}. Penning-ionization measurements showed a concomitant drop in the number density of $N_2(X,v)$. The reduced $N_2(B)$-state population appears, therefore, to result from $N_2(X,v)$ quenching rather than from quenching of $N_2(B)$ fluorescence by methane.

The relative $N_2(B)$ vibrational distribution, however, showed little variation with methane number density. This observation indicates that vibrational energy in the $N_2(A)$ does not have a major impact on the $N_2(B)$ vibrational distribution. A hotter vibrational distribution in the $N_2(X,v)$, on the other hand, does produce a hotter $N_2(B)$ vibrational distribution. Figure 5 illustrates this difference. The data points denoted by circles were taken under conditions where the $N_2(X,v)$ vibrational distribution could be characterized roughly by a vibrational temperature of 1800 K, and where only about 12% of the nitrogen was vibrationally excited. The points denoted as squares, however, were taken under conditions of a roughly 3700 K vibrational temperature of

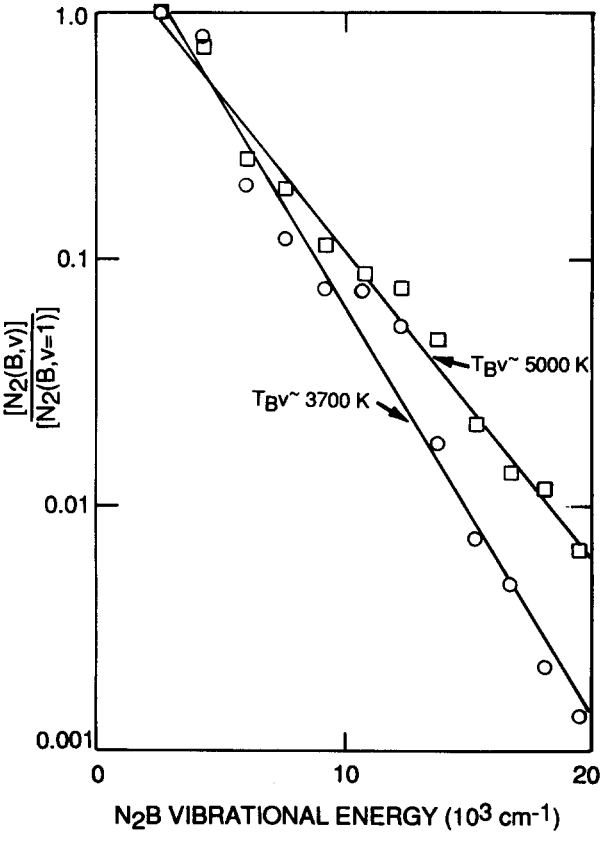

FIG. 5. Relative vibrational distributions for $N_2(B,v)$ for two different levels of $N_2(X,v)$ vibrational excitation. O: $T_{X''} \sim 1800$ K, $[N_2(X,v)]/[N_2(X)] \sim 0.12$; : $T_{X''} \sim 3700$ K, $[N_2(X,v)]/[N_2(X)] \sim 0.50$.

the $N_2(X,v)$ and with about 50% of the nitrogen vibrationally excited. Clearly the hotter ground-state distribution results in a hotter $N_2(B)$ distribution. The lines through the data points show for comparison Boltzmann distributions of the B state resulting from vibrational temperatures of 3700 and 5000 K.

A slight rearrangement of Eq. (6) gives the result

$$\frac{[N_2(B)]}{[N_2(A)]}\left\{1+\frac{k_3}{k_2}[N_2]+\frac{k_4}{k_2}[Q]\right\}=\frac{k_1}{k_2}[N_2(X,v)]. \tag{7}$$

Figure 6 shows the ratio of the $N_2(B)$ to $N_2(A)$ number densities, after correcting for quenching, plotted against the number density we estimate to be in vibrational levels 5–10 of the ground-electronic state. These vibrational levels are responsible for the bulk of the observed excitation. The number-density estimates were obtained from the Penning-ionization data with some extrapolation outside the region of greatest validity of the Penning-ionization diagnostic. While the data are somewhat scattered, they do indicate a clear trend with increasing $N_2(X,v)$ number density. The slope of the line through the data gives the result $k_1/k_2=(1.4\pm0.2)\times10^{-16}$ cm^3 molecule^{-1}. Given $k_2\sim2\times10^5$ s^{-1} we find the rate coefficient for exciting $N_2(B)$ in the interaction between $N_2(A)$ and $N_2(X,v)$ is 2.8×10^{-11} cm^3 molecule^{-1} s^{-1}. Given the uncertainties in the experimental data used to derive this value, we think a realistic value for k_1 is $(3.0\pm1.5)\times10^{-11}$ cm^3 molecule^{-1} s^{-1}.

If we assume that all $N_2(X)$ vibrational levels excite each energetically accessible $N_2(B)$ vibrational level with the same rate coefficient, we can estimate a distribution for the $N_2(X,v)$ by difference. That is, $N_2(B,v'=1)$ can be excited by $N_2(X,v\geqslant5)$, but excitation of $N_2(B,v'=2)$ is possible only from $N_2(X,v\geqslant6)$, and so on up to $N_2(B,v'=12)$ which requires $N_2(X,v\geqslant13)$. The $N_2(X,v)$ distribution obtained under these assumptions lies midway between modified Treanor and Boltzmann distributions with a common characteristic temperature. The modified Treanor distribution changes from a Treanor distribution for vibrational levels less than the Treanor minimum to one which varies as $1/v$ above the Treanor minimum. Our estimates of $N_2(X,v)$ number densities assume a modified Treanor distribution which the Penning-ionization measurements indicate is appropriate for vibrational levels 0–6. At some point the distribution should decrease more rapidly than $1/v$. Perhaps this increased drop off is reflected in $N_2(X,v)$ distribution estimated above to lie below a modified Treanor distribution. Equally likely, however, would be values of k_1 which varied with vibrational level. Without a more accurately determined $N_2(X,v)$ distribution, such variations cannot be determined.

B. Quenching of $N_2(A)$

Figure 7 shows how $N_2(A,v=0)$ varies as a function of time in the flow reactor in the absence and presence of

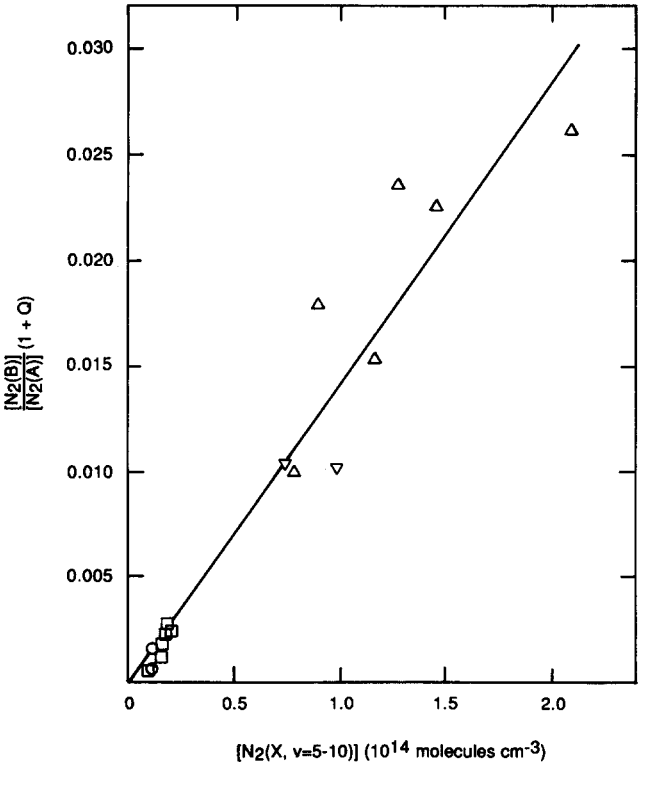

FIG. 6. Variation in the ratio of the number density of $N_2(B)$, after correcting for quenching, to that for $N_2(A)$ with the number density of $N_2(X,v=5\text{–}10)$.

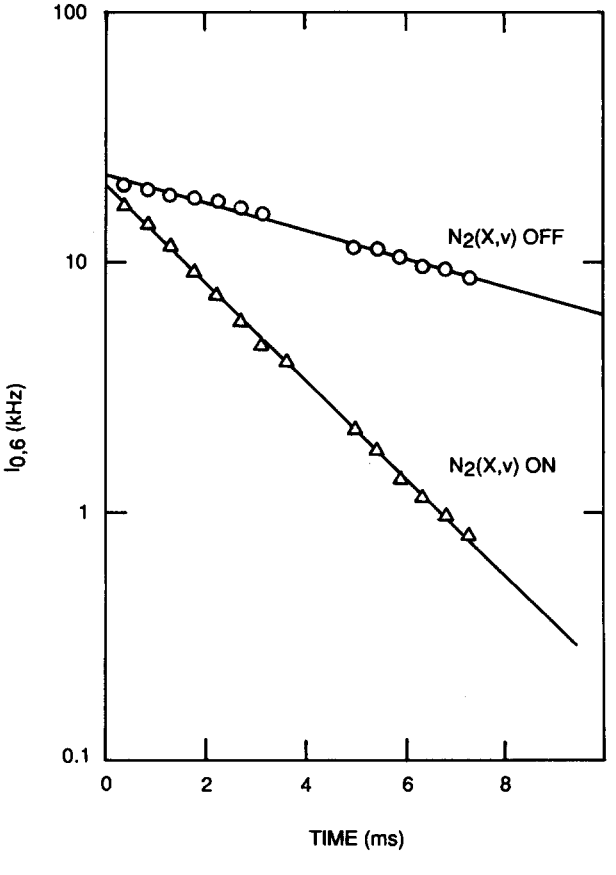

FIG. 7. Variation in intensity of the 0,6 Vegard–Kaplan band as a function of time in the absence and presence of $N_2(X,v)$.

$N_2(X,v)$. Clearly the $N_2(X,v)$ enhances the destruction of $N_2(A)$ dramatically. In the absence of $N_2(X,v)$, $N_2(A)$ decays principally by deactivation at the walls. When $N_2(X,v)$ enters the reactor, the $N_2(A)$ decay increases due to quenching by the $N_2(X,v)$ and perhaps a small amount of quenching from residual N atoms which did not recombine on the nickel screen. The relevant reactions are

$$N_2(A) + \text{wall} \rightarrow N_2(X) + \text{wall}, \tag{8}$$

$$N_2(A) + N_2(X,v) \rightarrow 2N_2(X), \tag{9}$$

$$N_2(A) + N \rightarrow N_2(X) + N(^2P). \tag{10}$$

An alternative to reaction (9) would be excitation to the B state followed by quenching out of the B state into the X state. Reaction (9), therefore, represents removal of molecules from the triplet manifold.

The rate equation describing these reactions is

$$\frac{d[N_2(A)]}{dt} = -\{k_8 + k_9[N_2(X,v)] + k_{10}[N]\} \times [N_2(A)]. \tag{11}$$

Under conditions such that the number densities of $N_2(X,v)$ and N remain essentially invariant with time, Eq. (11) has the solution

$$\ln\left\{\frac{[N_2(A)](t)}{[N_2(A)](t=0)}\right\} = -K_l t, \tag{12}$$

where the loss rate K_l is given by

$$K_l = 0.62\{k_8 + k_9[N_2(X,v)] + k_{10}[N]\}. \tag{13}$$

The factor of 0.62 corrects for the coupling of the radial number density gradient of $N_2(A)$ with the parabolic velocity profile in the reactor.[37–46] The semilog plot in Fig. 7 displays the expected linear behavior between the natural log of the $N_2(A)$ number density and the reaction time.

In the absence of $N_2(X,v)$, the decay of the metastables is determined principally by wall deactivation. This process is controlled by the rate of diffusion of the metastables to the walls. The wall-loss rate k_8 is given by[37]

$$k_8 = \frac{D_0 \lambda_0^2}{r^2 p}, \tag{14}$$

where D_0 is the diffusion coefficient in $cm^2\ s^{-1}$ at 1 Torr, λ_0 is the root of the zero-order Bessel function, 2.405, r is the flow tube radius, and p is the flow tube pressure. For the data in Fig. 7, the decay rate in the absence of $N_2(X,v)$ is $210\ s^{-1}$. This value agrees moderately well with the value of $180\ s^{-1}$ which we calculate from Eq. (14). We are unaware of experimental values for the diffusion coefficient of $N_2(A)$ in He. We used a value of $540\ cm^2\ s^{-1}$ at 1 Torr which we calculated for $N_2(X)$ in He using procedures described by Hirschfelder, Curtiss, and Bird.[47] The slight discrepancy could result from an incompletely developed flow profile in our reactor because of perturbations to the flow induced by the injectors or perhaps just increased surface area for deactivation because of the presence of the injectors.

The addition of $N_2(X,v)$ increases the decay rate of $N_2(A)$ to $731\ s^{-1}$. Since the N-atom number density is less than 10^{12} atoms cm^{-3}, and the rate coefficient for quenching $N_2(A)$ by N is $4.0\times10^{-11}\ cm^3\ molecule^{-1}\ s^{-1}$,[48] less than 10% of this increase in $N_2(A)$ decay can be attributed to quenching by atomic nitrogen. The balance, therefore, must result from quenching by $N_2(X,v)$. The rate of quenching $N_2(A)$ by $N_2(X,v)$ under the conditions of Fig. 7 is about $520\ s^{-1}$. From our Penning-ionization measurements we estimate an $N_2(X,v)$ number density of about 1.4×10^{14} molecules cm^{-3}. This value lets us estimate a quenching rate coefficient of $N_2(A)$ by $N_2(X,v)$ of about $3.7\times10^{-12}\ cm^3\ molecule^{-1}\ s^{-1}$. This is just over 10% of the previously estimated rate coefficient for reaction (1). The discrepancy between the two rate coefficients probably arises from the fact that little $N_2(A)$ is actually lost in pumping it from the A state to the B state. Most molecules pumped to the B state eventually return back to the A state via radiative or collisional cascade. Evidently some are lost by quenching out of the triplet manifold.

C. Regeneration of $N_2(A)$

Figure 8 shows direct evidence of this repopulation of the A state from pumping to the B state followed by cascade back to the A state. It shows the ultraviolet spectrum in the absence and presence of $N_2(X,v)$. The spectra were taken in the presence of methane, so that the $N_2(A)$ initially in the field of view was entirely in vibrational level 0. When the $N_2(X,v)$ mixes with the $N_2(A,v=0)$, however, vibrational levels 1 and 2 of the $N_2(A)$ are regenerated as is evident in Fig. 8(b).

The question arises as to whether the pumping of the $N_2(A,v)$ could be a direct excitation from $N_2(A,v=0)$ or if it is the result of cascade from the B state which has itself been pumped directly. We followed the time evolution of the ratio of the number densities of $N_2(A,v=1,2)$ to $N_2(A, v=0)$ to investigate this issue.

In the following discussion we will use a shorthand notation in which a nitrogen molecule in a specific vibronic state is identified by the letter of the electronic state with a superscript corresponding to the vibrational level in that state. For example, A^1 represents $N_2(A\ ^3\Sigma_u^+, v'=1)$.

In addition to reactions (1), (2), (8), and (9) the relevant reactions for $N_2(A,v=1)$ excitation and quenching include the following:

$$N_2(A,v=0) + N_2(X,v) \rightarrow N_2(A,v=1,2) + N_2(X,v), \tag{15}$$

$$N_2(A,v) + CH_4 \rightarrow N_2(A,v-1) + CH_4. \tag{16}$$

The rate of change in the number density of $N_2(A, v=1)$ with time is

$$\frac{d[A^1]}{dt} = \zeta_1 k_2[B] + k_{15}[A^0][X^v] + k_{16}^{v=2}[A^2][CH_4] - \{k_8 + k_9[X^v] + k_{16}^{v=1}[CH_4]\}[A^1], \tag{17}$$

where ζ_1 is the fraction of $N_2(B)$ excitations which cascade down to $N_2(A)$ vibrational level 1. Inserting Eq. (6) into Eq. (17) and rearranging gives the result

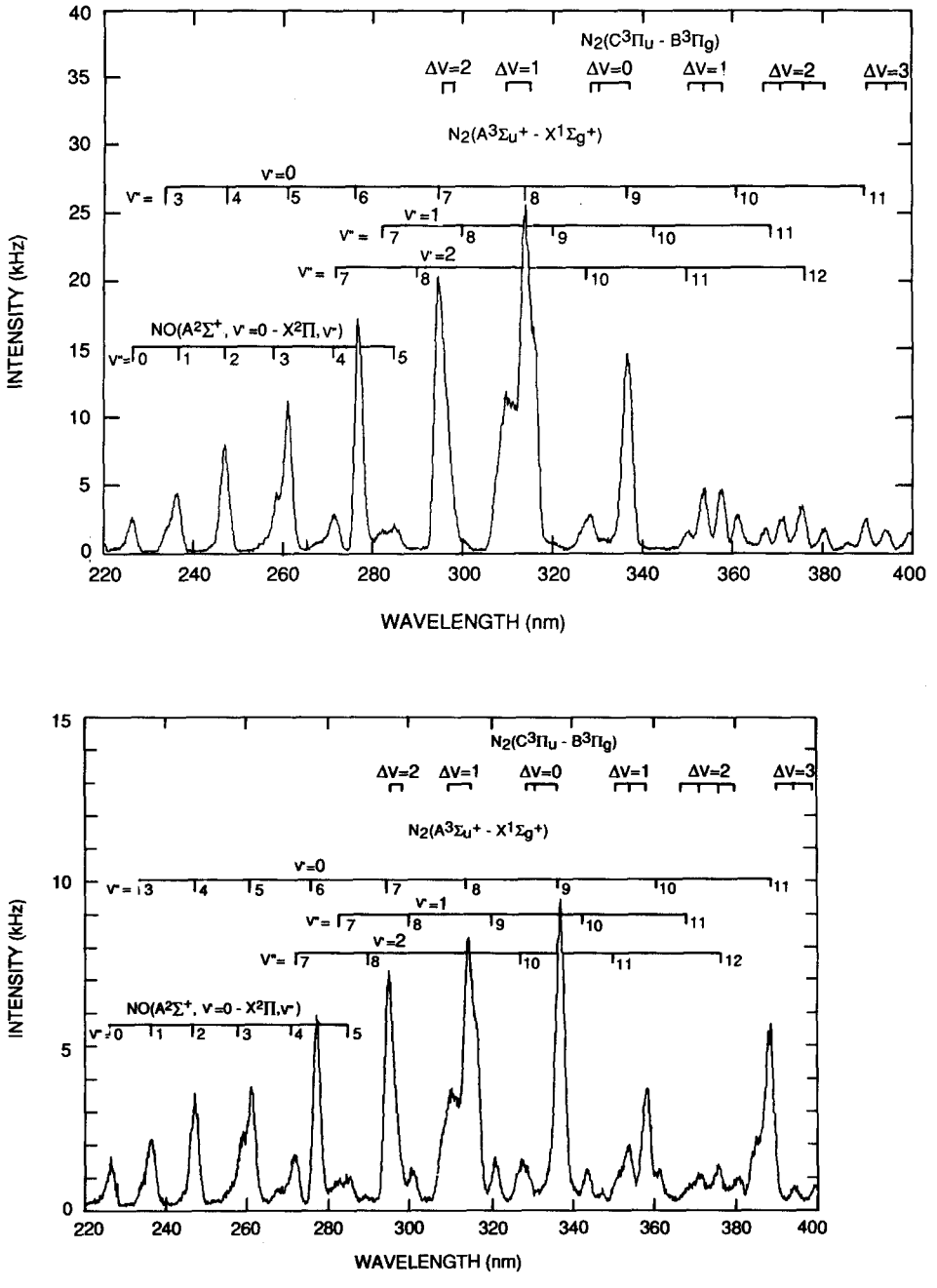

FIG. 8. (a) Spectrum of the nitrogen Vegard–Kaplan and second-positive, $N_2(C^3\Pi_u$–$B^3\Pi_g)$, bands in the presence of 6.1×10^{14} molecules cm^{-3} of methane, but the absence of $N_2(X,v)$. Note the absence of vibrationally excited $N_2(A)$ in the spectrum. (b) Spectrum of the nitrogen Vegard–Kaplan and second-positive bands in the presence of 6.1×10^{14} molecules cm^{-3} of methane and also in the presence of $N_2(X,v)$. Note the appearance of bands from vibrational levels 1 and 2 of the Vegard–Kaplan system.

$$\frac{d[A^1]}{dt} = \left[\frac{\zeta_1 k_1}{1+(k_3|k_2)[N_2]+(k_4|k_2)[Q]}+k_{15}\right][A^0][X^v] - \left\{k_8+k_9[X^v]+\left[k_{16}^{v=1}-k_{16}^{v=2}\frac{[A^2]}{[A^1]}\right][CH_4] - \left[1+\frac{[A^2]}{[A^1]}\right]\frac{\zeta_1 k_1[X^v]}{1+(k_3/k_2)[N_2]+(k_4/k_2)[Q]}\right\}\times[A^1]. \quad (18)$$

If the number–density ratio $[A^2]/[A^1]$ is constant, and if $[X^v]$ is constant, Eq. (18) can be solved analytically upon inserting the exponential form of Eq. (12) into it. The result is

$$\frac{[A^1]}{[A^0]} = \frac{K_f e^{-K_l^{v=0}t}}{K_l^{v=1}-K_l^{v=0}}\left\{1-e^{-[K_l^{v=1}-K_l^{v=0}]t}\right\}, \quad (19)$$

where we have made the substitutions for the formation and loss rates, K_f and K_l, respectively,

$$K_f = 0.62\left[\frac{\zeta_1 k_1}{1+(k_3/k_2)[N_2]+(k_4/k_2)[Q]}+k_{15}\right][X^v], \quad (20)$$

and

$$K_l^{v=1} = 0.62\left\{k_8+k_9[X^v]+\left[k_{16}^{v=1}-k_{16}^{v=2}\frac{[A^2]}{[A^1]}\right][CH_4]-\left[1+\frac{[A^2]}{[A^1]}\right]\times\frac{\zeta_1 k_1[X^v]}{1+(k_3/k_2)[N_2]+(k_4k_2)[Q]}\right\}. \quad (21)$$

Figure 9 shows the data plotted according to Eq. (19). The curve through the data is a least-squares fit. The result from the fit is $K_f = 174\ s^{-1}$ and $K_l^{v=1} = -184\ s^{-1}$.

Using the $N_2(B)$ vibrational distribution we observe from reaction (1), we calculate $\zeta_1 = 0.2$ and the ratio $[A^2]/[A^1] = 0.7$. These values agree quite well with our observations from this series of experiments. The rate coefficient for reaction (16) is 1.5×10^{-12} cm^3 molecule^{-1} s^{-1} for $v = 1$ and 3.1×10^{-12} cm^3 molecule^{-1} s^{-1} for $v = 2$.[26] Combining these values with the value of k_1, the quenching rate coefficients given above, and the number density for $N_2(X,v = 5$–$10)$ which we have estimated from Penning ionization measurements to be 1.4×10^{14} molecules cm^{-3}, we calculate a value for K_f of 280 s^{-1} if we neglect the direct excitation channel to produce $N_2(A,v = 1)$ from $N_2(A,v = 0)$. Assuming that k_8 and k_9 are the same for $v = 1$ as they were for $v = 0$, we calculate a value for $K_l^{v=1}$ of $-154\ s^{-1}$. Given the experimental uncertainties in this study, the much better than factor of two agreement between observed and calculated formation and loss rates must be considered quite good. This agreement doesn't preclude a direct excitation channel. Rather a direct excitation is not required to explain the observations.

IV. DISCUSSION

A. Mechanism

We have shown that the reaction between $N_2(A)$ and $N_2(X,v)$ results in efficient excitation of $N_2(B)$. The question arises as to whether the molecule originally in the A state is excited to the B state by the influx of the vibrational energy from the X-state molecule, or whether the X-state molecule is excited to the B state in an electronic-energy transfer from the A state. We think that the latter is more likely.

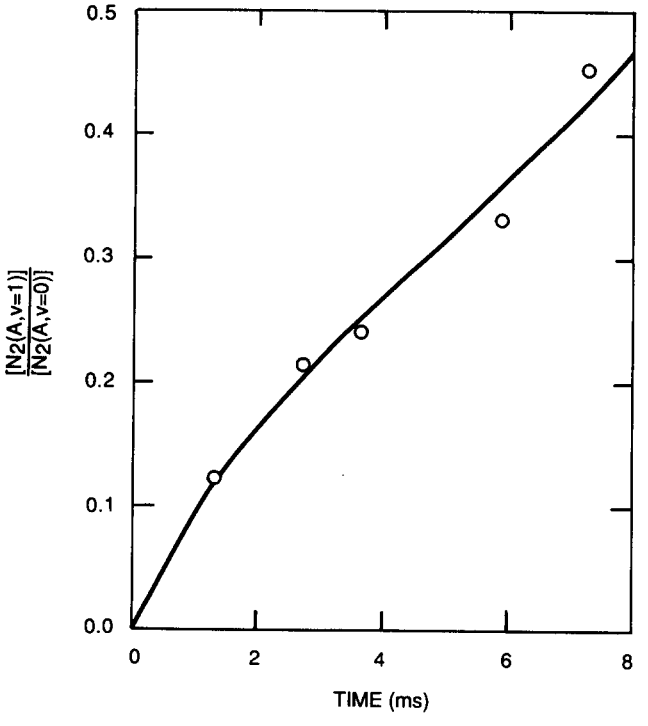

FIG. 9. Ratio of the number densities of $N_2(A,v = 1)$ to $N_2(A,v = 0)$ as a function of time. The line through the data is the least-square fit to Eq. (19).

One model that has become quite popular for rationalizing energy-transfer observations involves comparing rate coefficients with the product of the Franck–Condon factors of the two transitions involved in the energy transfer and multiplying that result by the absolute value of the energy defect of the reaction.[49–53] While we[23,28,54] and others[55,56] have shown on several occasions that this model is inadequate to describe the details of state-to-state observations, it may have some validity as a qualitative predictor.

For the case of direct excitation of the A state by the X state, we find that Franck–Condon factors coupling vibrational level 0 of the A state with various B-state vibrational levels become vanishingly small ($q_{v'v''} < 10^{-4}$) for transitions to B-state levels greater than $v = 5$. The implication, therefore, is that population rates of the higher B-state vibrational levels should be negligible. The higher vibrational B-state levels would be more readily excited from vibrationally excited $N_2(A)$. Thus where the A state excited directly to the B state one would see a strong dependence of the B-state vibrational distribution on that of the A state. This dependence is not observed.

The situation is markedly different for the case of electronic energy exchange. When $N_2(A,v = 0)$ transfers all of its energy to a given X-state level, the Franck–Condon factor coupling that level to the most nearly resonant B-state level is in all cases greater than 2×10^{-3}, and in most instances greater than 10^{-2}. The Franck–Condon factor coupling vibrational levels zero of the X and A states is small, 1×10^{-3}, but nonnegligible.

On the basis of just the Franck–Condon factors, the transfer appears even more facile if the A state does not give up all its energy in the transfer. For example, the collision between $N_2(A,v = 0)$ and $N_2(X, v = 16)$ to produce $N_2(X, v = 5)$ and $N_2(B,v = 8)$ has a Franck–Condon product three orders of magnitude greater than does the generation of $N_2(B,v = 8)$ and $N_2(X,v = 0)$ from the reaction between $N_2(X,v = 11)$ and $N_2(A,v = 0)$. This advantage will be offset somewhat by the lower number density in vibrational level 16 of the X state compared to that in vibrational level 11. The main point is that the Franck–Condon model appears to favor quite strongly the electronic-energy exchange channel.

The somewhat related observations of Pravilov *et al.*[53] demonstrate rather unequivocally that electronic-energy exchange does occur in collisions between ground-state and electronically excited nitrogen molecules. They studied the formation of the $N_2(B)$ state produced from N-atom recombination. Upon adding isotopically labeled nitrogen to their afterglow, they noted a strong shift in the positions of the first-positive bands. The observed fluorescence was from the isotopically labeled molecules which had been excited in an energy-transfer reaction with B-state molecules initially excited in the N-atom recombination.

B. Related studies

Hayes and Oskam[1] monitored the decays of $N_2(A)$ and $N_2(B)$ in the afterglow following a discharge pulse in a static

cell. They attributed the excitation of $N_2(B)$ to result primarily from energy pooling of two $N_2(A)$ molecules. They noted, however, that the variation in the ratios of the A state intensity to that of the B state was less than quadratic throughout the afterglow. Quadratic behavior would be expected in the event of excitation by $N_2(A)$ energy pooling. Furthermore, this deviation from quadratic behavior was greater for longer discharge pulses. They suggested reaction (1) as a second mechanism which might be responsible for some of the $N_2(B)$ excitation.

Our results show that reaction (1) is indeed efficient. Evidently, the longer discharge pulses in Hayes and Oskam's apparatus result in increased production of $N_2(X,v)$. The $N_2(B)$ excited from reaction (1) as opposed to the energy-pooling reaction, therefore, would become more and more significant as discharge-pulse lengths grew. Hayes and Oskam tried to eliminate the effects of reaction (1) by extrapolating their results to vanishingly small discharge-pulse lengths. The much larger value they reported for the energy-pooling reaction than that which we reported recently[28] indicates that they were not completely successful in this endeavor. Our energy-pooling results should not have been contaminated by reaction (1). Penning-ionization measurements of our $N_2(A)$ discharge source indicate an absence of $N_2(X,v)$.[6]

Over a number of years, Kenty[4,57–60] studied the orange afterglow resulting from passing current pulses through high pressure mixtures of rare gases containing a trace of nitrogen. He showed that these afterglows did not result from $N_2(B)$ excitation due to N-atom recombination, and suggested that the B state was excited by collisional transfer from a long-lived metastable in the afterglow. He proposed that this metastable was $N_2(W^3\Delta_u)$. Our results indicate that a more likely explanation for Kenty's observations is the energy-transfer reaction between $N_2(A)$ and $N_2(X,v)$. He did suggest this possibility himself in one of his later publications,[4] but even his last publication[60] championed $N_2(W)$ as being primarily responsible for his observations. Clearly the close coupling between the B and W states[32,61,62] means that the characteristics of the latter state might affect the observed B-state fluorescence. The primary excitation channel, however, is most likely reaction (1).

ACKNOWLEDGMENTS

We appreciate financial support from the Air Force Weapons Laboratories under Contract No. F29601-87-C-0056. Tom Tucker and Bill Cummings provided invaluable analytical support and George Caledonia, Dave Green, Terry Rawlins, and Bill Marinelli illuminated faint concepts. We thank Donna Samson, David Bastiani, Jeremy Piper, and Leo P. Kenney for suggestions on the text.

[1]G. N. Hayes and H. J. Oskam, J. Chem. Phys. **59**, 1507 (1973).
[2]Yu. A. Kulagin and L. A. Shelepin, Zh. Prikl. Spektrosk. **39**, 827 (1983).
[3]L. G. Piper and G. E. Caledonia, Bull. Am. Phys. Soc. **31**, 157 (1986).
[4]C. Kenty, *Proceedings of the Third International Conference on Physics of Electronic and Atomic Collisions*, edited by M. R. C. McDowell (North-Holland, Amsterdam, 1964), p. 1133.
[5]O. Dessaux, P. Goudmand, and B. Mutel, J. Quant. Spectrosc. Radiat. Transfer **30**, 311 (1983).
[6]L. G. Piper and W. J. Marinelli, J. Chem. Phys. **89**, 2918 (1988).
[7](a) L. G. Piper, PSI-1045/TR-755, prepared for the Air Force Weapons Laboratory under Contract No. F29601-87-C-0056 (1988); (b) L. G. Piper, PSI-1045/TR-790, prepared for the Air Force Weapons Laboratory under Contract No. F29601-87-C-0056 (1988); (c) L. G. Piper (in preparation).
[8]D. W. Setser, D. H. Stedman, and J. A. Coxon, J. Chem. Phys. **53**, 1004 (1970).
[9]D. H. Stedman and D. W. Setser, Chem. Phys. Lett. **2**, 542 (1968).
[10]A. L. Schmeltekopf, E. E. Ferguson, and F. C. Fehsenfeld, J. Chem. Phys. **48**, 2966 (1968).
[11]S. J. Young and K. P. Horn, J. Chem. Phys. **57**, 4835 (1972).
[12]C. R. Roy, J. W. Dreyer, and D. Perner, J. Chem. Phys. **63**, 2131 (1975).
[13]J. A. Michejda, L. J. Dubé and P. D. Burrow, J. Appl. Phys. **52**, 3121 (1981).
[14](a) F. Grum and G. W. Luckey, Appl. Opt. **7**, 2289 (1968); (b) F. Grum and T. E. Wightman, *ibid.* **16**, 2775 (1977).
[15]A. Fontijn, C. B. Meyer, and H. I. Schiff, J. Chem. Phys. **40**, 64 (1964).
[16]M. Vanpee, K. D. Hill, and W. R. Kineyko, AIAA J. **9**, 135 (1971).
[17]D. Golomb and J. H. Brown, J. Chem. Phys. **63**, 5246 (1975).
[18]G. A. Woolsey, P. H. Lee, and W. D. Slafer, J. Chem. Phys. **67**, 1220 (1977).
[19]M. Sutoh, Y. Morioka, and M. Nakamura, J. Chem. Phys. **72**, 20 (1980).
[20]A. M. Pravilov and L. G. Smirnova, Kinet. Catal. **19**, 202 (1978).
[21]G. Bradburn and H. Lilenfeld, J. Phys. Chem. **92**, 5266 (1988).
[22]L. G. Piper, G. E. Caledonia, and J. P. Kennealy, J. Chem. Phys. **75**, 2847 (1981).
[23]L. G. Piper, J. Chem. Phys. **88**, 231 (1988).
[24]D. E. Shemansky, J. Chem. Phys. **51**, 689 (1969).
[25]L. G. Piper, K. W. Holtzclaw, B. D. Green, and W. A. M. Blumberg, J. Chem. Phys. **90**, 5337 (1989).
[26]J. M. Thomas, J. B. Jeffries, and F. Kaufman, Chem. Phys. Lett. **102**, 50 (1983).
[27]L. G. Piper, W. J. Marinelli, W. T. Rawlins, and B. D. Green, J. Chem. Phys. **83**, 5602 (1985).
[28]L. G. Piper, J. Chem. Phys. **88**, 6911 (1988).
[29]E. E. Eyler and F. M. Pipkin, J. Chem. Phys. **79**, 3654 (1983).
[30]D. E. Shemansky, J. Chem. Phys. **64**, 565 (1976).
[31]K. B. Mitchell, J. Chem. Phys. **53**, 1795 (1970).
[32]A. Rotem and S. Rosenwaks, Opt. Eng. **22**, 564 (1983).
[33]W. Brennen and E. C. Shane, J. Phys. Chem. **75**, 1652 (1971).
[34]N. Jonathan and R. Petty, J. Chem. Phys. **50**, 3804 (1969).
[35]S. J. Davis and L. G. Piper (in preparation).
[36]K. D. Bayes and G. B. Kistiakowsky, J. Chem. Phys. **32**, 992 (1960).
[37]E. E. Ferguson, F. C. Fehsenfeld, and A. L. Schmeltekopf, *Advances in Atomic and Molecular Physics V*, edited by D. R. bates (Academic, New York, 1970).
[38]R. C. Bolden, R. S. Hemsworth, M. J. Shaw, and N. D. Twiddy, J. Phys. B **3**, 45 (1970).
[39]A. L. Farragher, Trans. Faraday Soc. **66**, 1411 (1970).
[40]R. W. Huggins and J. H. Cahn, J. Appl. Phys. **38**, 180 (1967).
[41]R. E. Walker, Phys. Fluids **4**, 1211 (1961).
[42]R. V. Poirier and R. W. Carr, J. Phys. Chem. **75**, 1593 (1971).
[43]M. Cher and C. S. Hollingsworth, Adv. Chem. Ser. **80**, 118 (1969).
[44]J. H. Kolts and D. W. Setser, J. Chem. Phys. **68**, 4848 (1978).
[45]M. J. Shaw and H. M. P. Stock, J. Phys. B **8**, 2752 (1975).
[46]A. R. DeSouza, G. Gousset, M. Touzeau, and Tu. Khiet, J. Phys. B **18**, L661 (1985).
[47]J. O. Hirschfelder, C. F. Curtiss, and R. B. Bird, *Molecular Theory of Gases and Liquids* (Wiley, New York, 1964).
[48]L. G. Piper, J. Chem. Phys. (in press).
[49]I. Deperasinska, J. A. Beswick, and A. Tramer, J. Chem. Phys. **71**, 2477 (1979).
[50]R. D. Coombe and C.H-T. Lam, J. Chem. Phys. **80**, 3106 (1984).
[51]D. H. Katayama, T. A. Miller, and V. E. Bondybey, J. Chem. Phys. **72**, 5469 (1980).
[52]J. Herbelin, Chem. Phys. Lett. **133**, 331 (1987).
[53]A. M. Pravilov, L. G. Smirnova, and A. F. Vilesov, Chem. Phys. Lett. **144**, 469 (1988).
[54]L. G. Piper, L. M. Cowles, and W. T. Rawlins, J. Chem. Phys. **85**, 3369 (1986).
[55]D. H. Katayama, A. V. Dentamaro, and J. A. Welsh, J. Chem. Phys. **87**, 6983 (1987).

[56]G. Jihua, A. Ali, and P. J. Dagdigian, J. Chem. Phys. **85**, 7098 (1986).
[57]C. Kenty, Phys. Rev. **89**, 336 (1953).
[58]C. Kenty, J. Chem. Phys. **23**, 1555 (1955).
[59]C. Kenty, J. Chem. Phys. **41**, 3996 (1964).
[60]C. Kenty, J. Chem. Phys. **47**, 2545 (1967).
[61]A. Rotem, I. Nadler, and S. Rosenwaks, Chem. Phys. Lett. **83**, 281 (1981).
[62]N. Sadeghi and D. W. Setser, J. Chem. Phys. **79**, 2710 (1983).